

# An improved But Reliable Model for MESFET Parasitic Capacitance Extraction

B. L. Ooi and J. Y. Ma

**Abstract--** The conventional parasitic capacitance extraction always produces bias-dependent  $C_{pd}$ , even though from the underlying physic, the parasitic capacitance is known to be bias-independent. In this paper, an improved model is thus proposed to evaluate the parasitic capacitances of GaAs MESFET transistor from the cold-FET S-parameters measurement. The resulting  $C_{pd}$  is found to be independent of  $V_{gs}$ , when  $V_{gs} < V_p$ . In our approach, model parameters can be uniquely determined by using only two sets of cold-FET S-parameters under different  $V_{gs}$  biasing condition.

**Index Terms--**Small Signal Equivalent Circuit

## I. INTRODUCTION

The small signal equivalent circuit of MESFET is very useful for device performance analysis and microwave circuit design. A typical small signal equivalent circuit of the microwave MESFET is shown in Fig. 1. It consists of the intrinsic elements, which are enclosed by the dashed-box as shown in Fig. 1, and the extrinsic parasitic elements, which include the element  $R_s$ ,  $R_g$ ,  $R_d$ ,  $L_s$ ,  $L_g$ ,  $L_d$ ,  $C_{pg}$  and  $C_{pd}$ . The intrinsic components are usually calculated after a de-embedding process through which the effect of the parasitics is removed. As such, it becomes very crucial that all external parasitics be accurately determined.

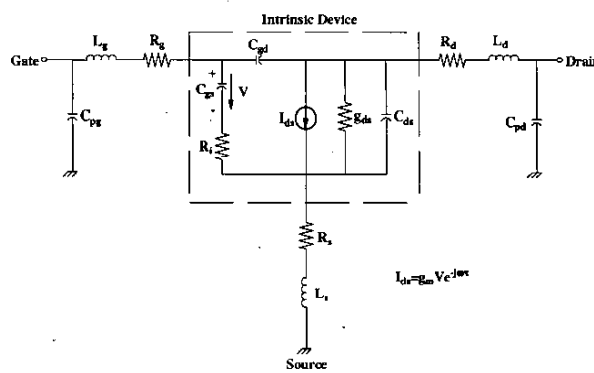


Fig. 1. MESFET small-signal equivalent circuit

The determination of the parasitic capacitances is always based on the measured Y-parameters at the gate bias beyond the pinch-off voltage ( $V_{gs} < V_p$ ), and with both the

source and the drain grounded ( $V_{ds}=0$ ). Fig. 2 shows the Y-parameters of a  $2*150\mu\text{m}$  MESFET device. As noted from the figure, when the frequency is low, the influence of the parasitic resistances and inductances on the imaginary parts of the Y-parameters,  $\text{Im}(Y_{ij})$ , can be neglected. The imaginary parts of the Y parameters can be taken to be caused by the capacitive effect. Based on this assumption, two models are commonly used for estimating  $C_{pg}$  and  $C_{pd}$  [1] & [2].

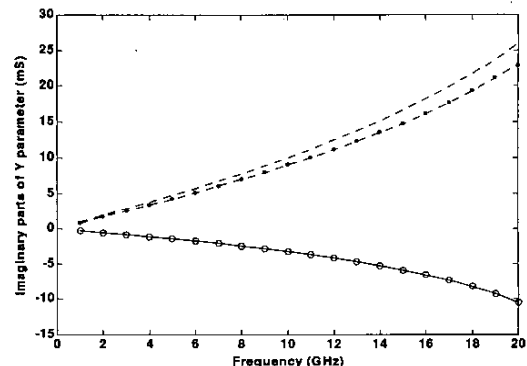


Fig. 2. Imaginary parts of Y parameters versus frequency. Measured at  $V_{ds}=0$ ,  $V_{gs}=-5.0$ ,  $V_{gs} < V_p$ ,  $0.5\mu\text{m}$ ,  $2*150\mu\text{m}$  MESFET (---  $Y_{11}$ , —  $Y_{12}$ , ○○○  $Y_{21}$ , -·-·-  $Y_{22}$ )

## II. DAMBRINE'S MODEL[1]

The equivalent circuit of the Dambrine's model is shown in Fig. 3. The model assumes that under cold-FET condition with  $V_{gs}$  biased at pinch-off region, the depletion region beneath the gate can be modeled by two capacitors with the same value,  $C_b$ , which is the fringing capacitance due to depletion layer extension at each side of the gate. At low frequency, the imaginary parts of the Y parameter can thus be written as:

$$\text{Im}(Y_{11}) = j\omega(C_{pg} + 2 \cdot C_b), \quad (1)$$

$$\text{Im}(Y_{12}) = \text{Im}(Y_{21}) = -j\omega C_b, \text{ and} \quad (2)$$

$$\text{Im}(Y_{22}) = j\omega(C_b + C_{pd}). \quad (3)$$

Hence, the elements  $C_{pg}$  and  $C_{pd}$  can be extracted from

$$C_{pg} = \frac{\text{Im}(Y_{11}) + 2 \text{Im}(Y_{12})}{j\omega}, \text{ and} \quad (4)$$

The authors are with the Department of Electrical and Computer Engineering, National University of Singapore, 10 Kent Ridge Crescent, Singapore 119260. Email: eleooib@nus.edu.sg ; Fax:67791103

$$C_{pd} = \frac{\text{Im}(Y_{22}) + \text{Im}(Y_{12})}{\omega}. \quad (5)$$

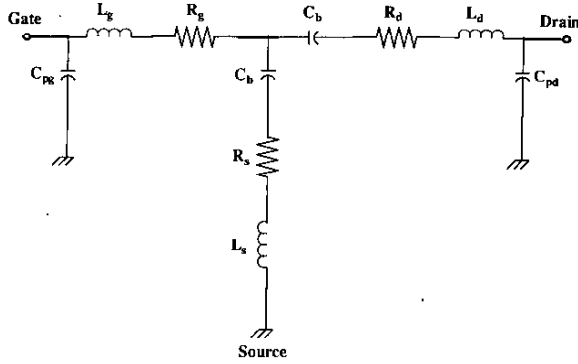


Fig. 3. Small-signal equivalent circuit at  $V_{ds}=0$  and  $V_{gs} < V_p$  for Dambrine's model.

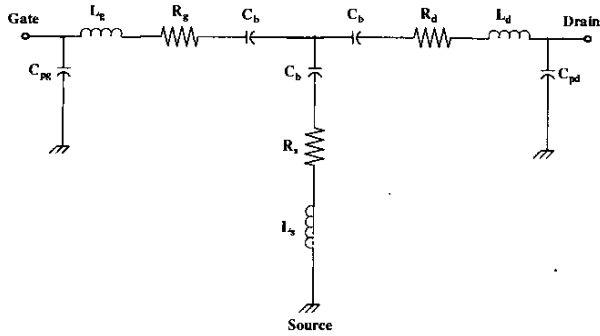


Fig. 4 White's small-signal equivalent circuit model at  $V_{ds}=0$  and  $V_{gs} < V_p$ .

### III. WHITE'S MODEL [2]

The equivalent circuit of the White's model is shown in Fig. 4. The depletion region under the gate is modeled by three re-defined identical capacitors  $C_b$ , connecting to gate, source and drain respectively. The connecting node can be explained as a hypothetical point within the depletion region. It is positioned in such a way so that the capacitances with respect to the gate, the drain and the source are all equal. When frequency is low, the imaginary parts of the  $Y$  parameter can be written as:

$$\text{Im}(Y_{11}) = j\omega(C_{pg} + \frac{2}{3}C_b), \quad (6)$$

$$\text{Im}(Y_{12}) = \text{Im}(Y_{21}) = -j\omega \frac{C_b}{3}, \text{ and} \quad (7)$$

$$\text{Im}(Y_{22}) = j\omega(2 \cdot C_b + \frac{2}{3}C_{pd}). \quad (8)$$

The capacitances  $C_{pg}$  and  $C_{pd}$  are determined from

$$C_{pg} = \frac{\text{Im}(Y_{11}) + 2 \text{Im}(Y_{12})}{\omega}, \text{ and} \quad (9)$$

$$C_{pd} = \frac{\text{Im}(Y_{22}) + 2 \text{Im}(Y_{12})}{\omega}. \quad (10)$$

As noted from the above equations, both models yield the same results for the parasitic capacitance  $C_{pg}$ . However, different expressions are obtained for the capacitance  $C_{pd}$  under the two models.

To study the problem in greater detail, the cold FET S-parameters are measured for a  $2*100\mu\text{m}$  and a  $2*150\mu\text{m}$  MESFET devices. For both devices, the measurements are made under three different  $V_{gs}$  bias points, all beyond pinch-off, with  $V_{ds}=0$ . Parasitic capacitances  $C_{pg}$  and  $C_{pd}$  are computed using these measured data for both the Dambrine's and White's Model. The result is depicted in Fig. 9.

As observed from Fig. 9, the extracted  $C_{pg}$  remains relatively constant under different  $V_{gs}$  bias condition (all beyond pinch-off) for both Dambrine's and White's model. Both transistors give similar trend for the extracted  $C_{pg}$ . This result is in agreement with the bias independent nature of the parasitic capacitance  $C_{pg}$ .

From Fig. 9, it is also noted that the extracted  $C_{pd}$  under different bias conditions varies widely for the two models. As seen from the figure, the White's model has the largest variation in the extracted  $C_{pd}$  as compared to the Dambrine's model. Both transistors show similar trend for the extracted  $C_{pd}$ . The extracted  $C_{pd}$  values from both models are in violation with the bias independent nature of the parasitic capacitance. Thus, a more accurate and reliable extraction technique for the capacitance  $C_{pd}$  is needed.

### IV. THE PROPOSED MODEL

Fig. 5 shows the equivalent circuit of our improved model for MESFET biasing at  $V_{gs} < V_p$  and  $V_{ds}=0$ . The depletion region under the gate is modeled by three  $\Pi$  capacitors, connected from the gate to the source  $C_f$ , from the gate to the drain  $C_f$ , and between drain and source  $\alpha C_f$ . The proposed model can be transformed into a TEE topology and this is depicted in Fig. 6. The physical origin of the new model elements is illustrated in Fig. 7, in which the depletion region is described by three capacitances associated with gate, drain and source. The connecting point P can be taken as a hypothetical node within the depletion region. An additional parameter  $\alpha$  is introduced to adjust the location of P such that the capacitances from P to gate, source and drain are  $(2+1/\alpha)C_f$ ,  $2(2+1/\alpha)C_f$  and  $2(2+1/\alpha)C_f$  respectively. It can be seen that the capacitances from P to drain and source are the same, while the capacitance from P to gate has a different value.

When frequency is low, the imaginary parts of the  $Y$  parameters can be written as:

$$\text{Im}(Y_{11}) = j\omega(C_{pg} + 2 \cdot C_f), \quad (11)$$

$$\text{Im}(Y_{12}) = \text{Im}(Y_{21}) = -j\omega C_f, \text{ and} \quad (12)$$

$$\text{Im}(Y_{22}) = j\omega(C_{pd} + C_f + \alpha C_f). \quad (13)$$

Hence, both  $C_{pg}$  and  $C_{pd}$  can be determined from

$$C_{pg} = \frac{\text{Im}(Y_{11}) + 2 \text{Im}(Y_{12})}{\omega}, \text{ and} \quad (14)$$

$$C_{pd} = \frac{\text{Im}(Y_{22}) + (1 + \alpha) \text{Im}(Y_{12})}{\omega}. \quad (15)$$

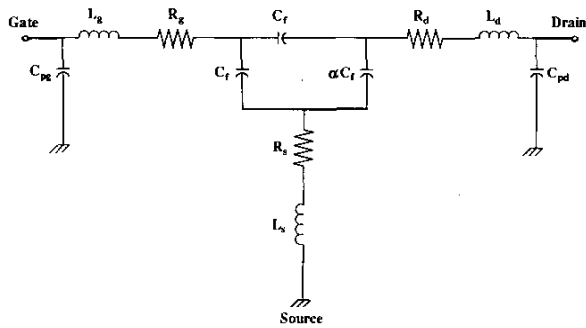


Fig. 5. Equivalent circuit of the improved model for MESFET biasing at  $V_{gs} < V_p$  and  $V_{ds} = 0$ , intrinsic elements in  $\Pi$  topology

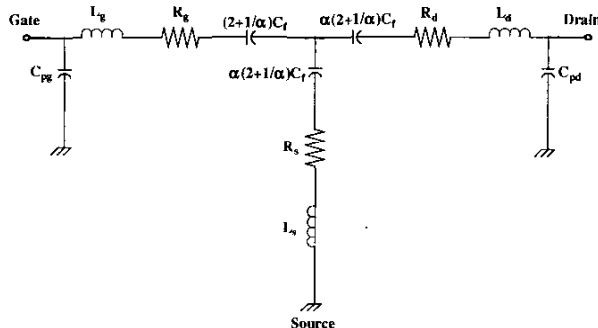


Fig. 6. Equivalent circuit of the improved model for MESFET biasing at  $V_{gs} < V_p$  and  $V_{ds} = 0$ , intrinsic elements in TEE topology

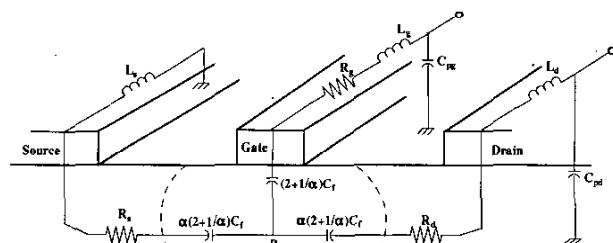


Fig. 7. Cross section view of MESFET at  $V_{gs} < V_p$  and  $V_{ds} = 0$ , showing physical origin of the improved model

The parameter  $\alpha$  in equations (13) and (15) is an additional parameter for modeling, and it can be determined through the procedures described below.

Assuming  $YA$  is the Y-parameter from the cold-FET measurements for  $V_{gs} = V_{gs1} < V_p$ , and  $V_{ds} = 0$ ,  $YB$  is the Y-parameter from cold-FET measurement for  $V_{gs} = V_{gs2} < V_p$ , and  $V_{ds} = 0$ , we have the following equations:

$$\text{Im}(YA_{22}) = j\omega(C_{pd} + C_f + \alpha C_f), \quad (16)$$

$$= j\omega C_{pd} - (1 + \alpha) \text{Im}(YA_{12}),$$

$$\text{Im}(YB_{22}) = j\omega(C_{pd} + C_f + \alpha C_f), \quad \text{and} \quad (17)$$

$$= j\omega C_{pd} - (1 + \alpha) \text{Im}(YB_{12}),$$

$$\alpha = \frac{\text{Im}(YA_{22}) - \text{Im}(YB_{22})}{\text{Im}(YB_{12}) - \text{Im}(YA_{12})} - 1. \quad (18)$$

Numerous experimentations have been conducted and the results show that the computed  $\alpha$  is independent on the two  $V_{gs}$  values chosen. A typical result is shown in Fig. 8. As noted from the figure, using different cold-FET pinch-off measurement data would yield approximately the same  $\alpha$  value.

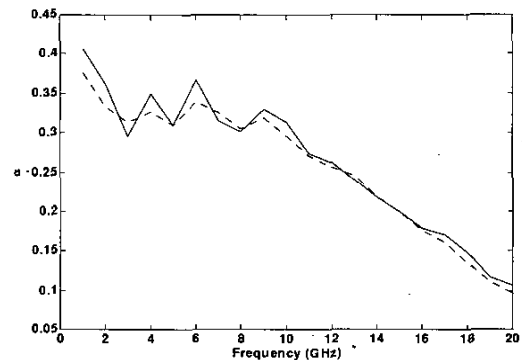


Fig. 8. Calculated  $\alpha$  using different  $V_{gs}$  ( $V_{gs} < V_p$ ) value, (---  $\alpha$  calculated with cold-FET S-parameter of  $V_{gs} = -5.0V$  and  $V_{gs} = -2.0V$ , —  $\alpha$  calculated with cold-FET S-parameters of  $V_{gs} = -5.0V$  and  $V_{gs} = -1.7V$ )

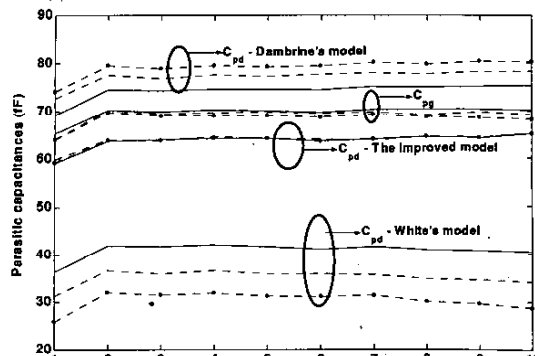
## V. VERIFICATION OF THE PROPOSED MODEL

The same  $2*100\mu\text{m}$  and  $2*150\mu\text{m}$  MESFET devices are adopted for investigation. The pinch-off voltages of the devices are  $-1.2\text{V}$  and  $-1.23\text{V}$  respectively. The cold-FET S-parameters are measured under three different  $V_{gs}$  bias voltages, namely,  $-5.0\text{V}$ ,  $-2.0\text{V}$  and  $-1.7\text{V}$ .

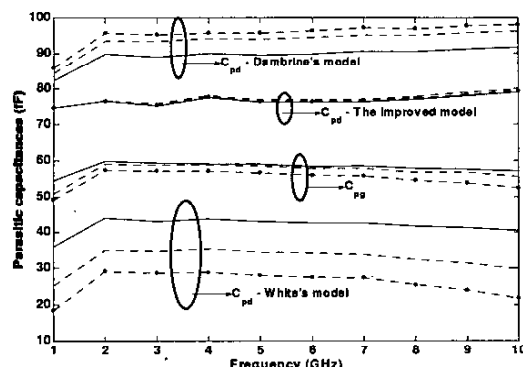
The extracted parasitic capacitances  $C_{pg}$  and  $C_{pd}$  are plotted in Figures 9(a) and 9(b). The results obtained from the Dambrine's model, and the White's models are also enclosed for comparison.

It can be seen from Fig. 9 that the calculated  $C_{pd}$  value using the improved model does not change with  $V_{gs}$ . The RMS variation of the calculated  $C_{pd}$  under the three different  $V_{gs}$  bias using Dambrine's model, White's model and the improved model is listed in Table 1. Of all the models, the proposed model has the lowest RMS variation in  $C_{pd}$ .

Based on the parasitic capacitances calculated from the improved model, the other small signal equivalent circuit parameters for the  $2*100\mu\text{m}$  device are computed. A good agreement between the measured and modeled S-parameters are obtained in Fig. 10.



(a)



(b)

Fig. 9. Calculated parasitic capacitances by Dambrine's model, White's model and the improved model under three different biasing conditions ( $V_{ds}=0$ , —  $V_{gs}=-5.0$ , - - -  $V_{gs}=-2.0V$ , - -  $V_{gs}=-1.7V$ ), (a)  $2*100\mu m$  MESFET (b)  $2*150\mu m$  MESFET.

2*100 $\mu m$			2*150 $\mu m$		
Dambrine model	White model	Proposed model	Dambrine model	White model	Proposed model
4.91%	10.6%	0.32%	6.14%	15.86%	0.67%

Table 1. The RMS variation of the calculated  $C_{pd}$  under three different  $V_{gs}$  bias conditions using Dambrine's model, White's model and the proposed model (1-10GHz).

## VI. CONCLUSION

An improved and reliable model for extracting MESFET parasitic capacitance  $C_{pg}$  and  $C_{pd}$  is proposed. It is noted that the conventional parasitic extraction method gives non-physical  $C_{pd}$  value. By introducing a new capacitor in modeling the depletion region under the gate, the improved model gives accurate estimation for  $C_{pd}$ , and the result is observed to be independent of  $V_{gs}$  biasing voltage.

## VII. REFERENCES

1. G. Dambrine, A. Cappy, F. Heliodore, and E. Playez, "A new method for determining the FET small-signal

equivalent circuit," IEEE Trans. Microwave Theory Tech., vol. 36, no. 7, pp.1151-1159, July 1988

2. J.A.Reynoso-Hernandez, B. Ramirez-Duran, J. Ibarra-Villasenor, and J. Perdomo, "Reliable RF techniques for extracting parasitic elements in microwave FET's", International IEEE Workshop on Experimentally Based  $2*100\mu m$  FET Device Modelling & Related Nonlinear Circuit Design, 1996.
3. J.A. Reynoso-Hernandez, F.E. Rangel-Patino, and J. Perdomo, "Full RF Characterization for Extracting the Small-Signal Equivalent Circuit in Microwave FET's", IEEE Transactions on Microwave Theory and Techniques, vol. 44, no.12, December 1996.
4. Paul M. White, Richard M. Healy "Improved Equivalent Circuit for Determination of MESFET and HEMT Parasitic Capacitances from "Coldfet" Measurements", IEEE Microwave and Guided Wave Letters, vol. 3, no.12, pp. 453-454, December 1993

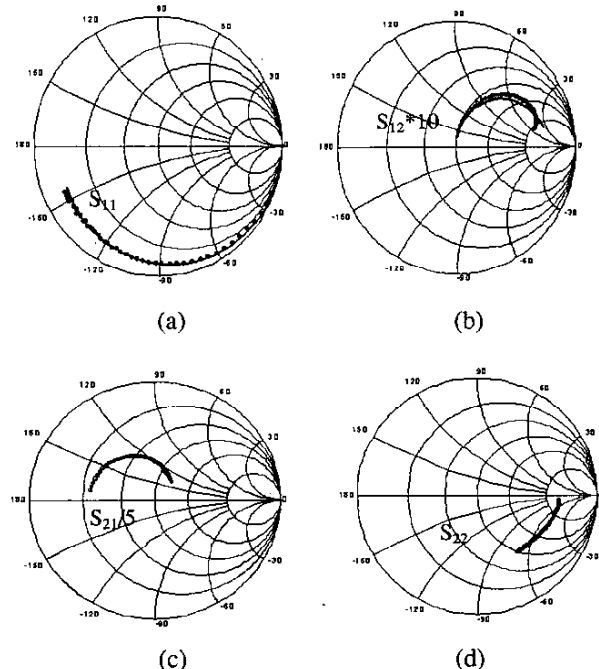


Fig. 10. Comparison between modeled and measured S-parameter,  $V_{gs}=0.4V$ ,  $V_{ds}=5.0V$ , (a)  $S_{11}$ , (b)  $S_{12}*10$ , (c)  $S_{21}/5$ , (d)  $S_{22}$ , (— Modeled  $S_{11}$ ,  $S_{12}$ ,  $S_{21}$ ,  $S_{22}$ , ○○○ Measured  $S_{11}$ ,  $S_{12}$ ,  $S_{21}$ ,  $S_{22}$ )